The analysis and performance of the Inverted-Coaxial Point-Contact detectors in the MAJORANA DEMONSTRATOR experiment

J.M.López-Castaño on behalf of the MAJORANA Collaboration

U.S. DEPARTMENT OF ENERGY | Office of Science
NSF
Sanford Underground Research Facility

1. INTRODUCTION

- The MAJORANA DEMONSTRATOR: modular array to search for $0\nu\beta\beta$ and show the feasibility of a 1-ton experiment.
- After the success of MAJORANA and GERDA experiments, their technology forms the basis of the Large Enriched Germanium Experiment for Neutrinoless $\beta\beta$ Decay (LEGEND) program.

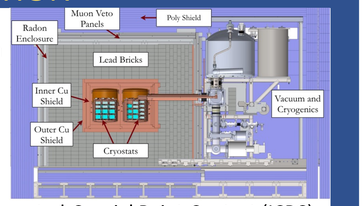

- LEGEND will use the new Inverted-Coaxial Point-Contact (ICPC) detector design, which is a larger mass evolution of the detectors previously adopted by MAJORANA and GERDA.
- The ICPC detectors were installed for the final run of the DEMONSTRATOR from August 2020 to March 2021.
- Larger ICPC crystal size result in long drift times, and hence a greater charge trapping effects. This led us to develop an improved correction based on the measured drift time.

2. WAVEFORM FEATURES

The $0\nu\beta\beta$ analysis and background discrimination is based on 6 parameters representing the germanium detector waveform

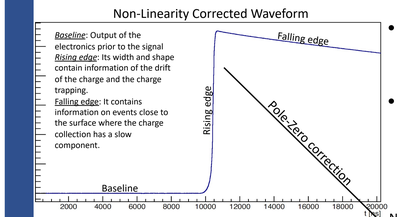

- 1 parameter is obtained from fitting the falling edge of the non-linearity corrected waveform:
  - $\underline{\lambda}$: Slope of a linear fit to the falling edge
- The charge collected during the rising edge is dissipated by the electronic RC circuit in the falling edge. A Pole-Zero correction is applied to the waveform to flatten the falling edge.

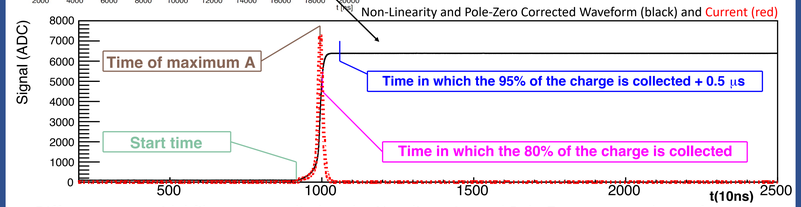

- Different trapezoidal filters are applied to the Non-linearity and Pole-Zero corrected waveform to extract different information:
  - Energy: The height of the pulse above the baseline relates to the total collected energy
  - Drift time-charge (DT): The time of charge collection (width of the rising edge) and the shape of the pulse in that time are correlated with the length of time the charges are drifting within the detector.
  - A: The derivate of the rising edge yields the maximum current of the pulse.
  - DCR: Change in the height of the pulse during the Pole-Zero corrected falling edge. Both, DCR and λ, provides a measure of the charge collected after the rising edge. While λ is calculated across the falling edge, DCR is evaluated between two regions of the pole-zero corrected falling edge.
  - LQ: The time to collect the final 20% of the charge and shape of the pulse in this region determines the late charge parameter

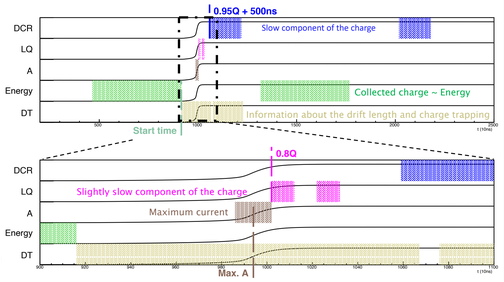

Top: 5 rows with the Non-linearity Pole-Zero corrected waveform. Each row repeats the same charge pulse and contains shaded regions corresponding with the trapezoidal filter for each variable. Each trapezoidal filter is formed by two regions separated by the trapezoidal flat time. The first region corresponds to the fall time, while the second region cover the rise time. The reference time for placing the regions in the energy, DT and DCR are indicated. Bottom: Zoom of the top panel, including the refence time for placing the trapezoidal regions in A and LQ.

3. ENERGY DETERMINATION

- The energy estimation is correlated with DT and λ.
- The energy resolution improves after correcting for these correlations: 3 possible corrections can be found for the following distributions.

EXAMPLES FROM DETECTOR P43406A: CALIBRATION DATA SURROUNDING THE 2614.5 keV peak from ^{208}Tl

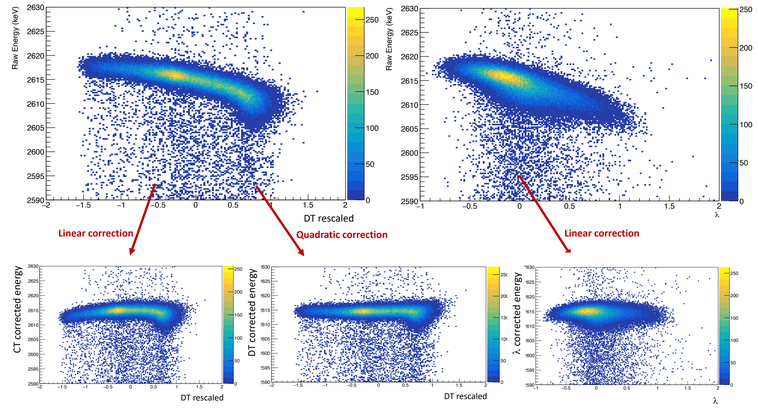

- Combining corrections based on DT with the correction based in λ, two new energy parameters are obtained to get a total of 5 possible energy-corrected parameters.
- The correction method that yields the best energy resolution is used, though the selection varies by detector.
- The energy corrections are found to be stable in time (<0.4 keV) across all calibrations.

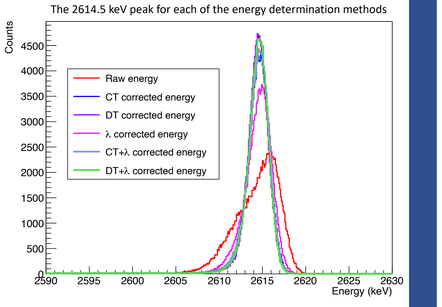

The energy resolution level of the ICPC detectors are competitive with the energy resolution previously obtained from P-type Point-Contact detectors

4. PULSE SHAPE ANALYSIS

- 4 different cuts are used to remove backgrounds based on the topology of the event.
  - *Low A/E cut*: Remove multi-site events where the current amplitude of a single interaction is reduced relative to the total charge.
  - *High A/E cut*: Remove α events near the Point-Contact with an enhanced current amplitude.
  - *DCR cut*: Remove α backgrounds near the passive surface due to the delayed charge component after the rising edge.
  - *LQ/E cut*: Remove 1) multi-site events where one interaction is near the Point-Contact where the current amplitude is not reduced enough to be rejected by the Low A/E cut, and 2) events with a slightly slow component of the charge due to partial energy deposition in the transition region of the dead-layer.
- The raw values for A/E, DCR and LQ/E are correlated with DT.
- The background rejection performance of the cuts improve after applying a DT correlation.

Correlation between DCR and DT

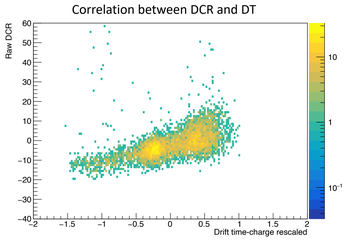

Correlation between Raw A/E and DT

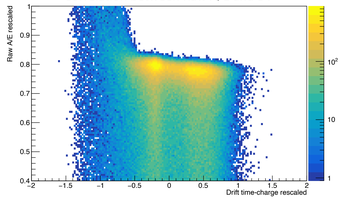

Correlation between LQ and DT

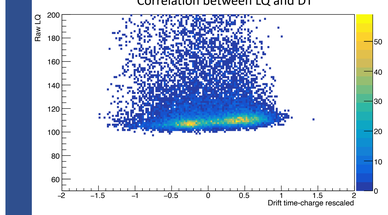

- The A/E value after DT correction is slightly correlated with the energy.
  - Its correction slightly improve the background rejection.

Correlation between DT-corrected A/E and energy

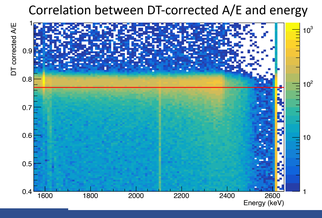

- The background rejection cut values are chosen based on the acceptance of the cut
  - A/E distribution for the Double Escape Peak of the 2614.5 keV γ is used to set the Low A/E cut in a value below the A/E peak with 95% acceptance. The high A/E is placed above the A/E peak at a distance that is twice that to the low A/E cut.
  - DCR distribution of the Compton continuum is rescaled to follow a gaussian of mean 0 and sigma 1 and the cut is chosen at 3 (=3σ of acceptance)
  - LQ/E distribution of the Compton continuum is rescaled to follow a gaussian of mean 0 and sigma 1 and the cut is chosen at 5 (=5σ of acceptance)
- The stability of the analysis is determined by observing the change in the parameters.
  - Parameters used to find the final value of A/E, DCR or LQ/E.
  - Parameters to set the cuts: Peak position in the distribution and Cut position respect the peak.
- When the distance between the A/E peak position and cut changes more than 1.5 times, the background data in between is rejected.

Example of stability plot: stability plot for A/E parameters where a period of time is rejected in the analysis.

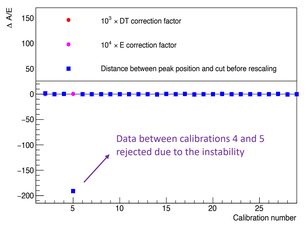

5. RESULTS

DETECTOR	ENERGY RESOLUTION: FWHM (keV)		
	Raw E at 2614.5 keV	Corrected E at 2614.5 keV	Corrected E at $Q_{\beta\beta}$
P43406A	4.9	3.02	2.41
p43415A	7.8	3.12	2.60
P43387A	5.5	2.89	2.33
P43389A	8.4	3.36	2.71

Table: ICPC features. The columns corresponds to 1) the detector serial number, 2) energy resolution measured at the 2614.5 keV peak in the ^{228}Th calibration data for ICPC detectors before any correction was applied, 3) same energy resolution after the best correction was chosen and applied 4) energy resolution after the best correction at $Q_{\beta\beta}$, and 5) the background index measured in the ICPC detectors.

More details about the neutrinoless double beta decay MAJORANA analysis including the ICPC detectors in the poster:
"The analysis and new results from the full dataset of the MAJORANA DEMONSTRATOR" by I.Guinn, A.Hostiuc, T.Oli, and N.W.Rouf

The Majorana Collaboration: Franklin Adams, Isaac Arnquist, Frank Avignone, Alexander Barabash, CJ Barton, Kevin Bhimani, Ethan Blalock, Brady Bos, Matthew Busch, Micah Buuck, Thomas Caldwell, Ana Carolina, Yuen-Dat Chan, Cabot-Ann Christofferson, Pinghan Chu, Morgan Clark, Clara Cuesta, Jason Detwiler, Maria-Laura di Vacri, Yuri Efremenko, Hiroyasu Ejiri, Steven Elliott, Aaron Engelhardt, Rushabh Gala, Graham Giovanetti, Matthew Green, Julieta Gruszko, Ian Guinn, Vincente Guiseppe, Chris Haufe, Reyco Henning, David Hervas, Eric Hoppe, Alexandru Hostiuc, Mary Kidd, Inwook Kim, Richard T. Kouzes, Thomas Lannen, Aobo Li, José Mariano López-Castaño, Eric Martin, Ryan Martin, Ralph Massarczyk, Samuel Meijer, Susanne Mertens, Tupendra Oli, Gulden Othman, Laxman Paudel, Jessica Peterson, Walter Pettus, Alan Poon, David Radford, Anna Reine, Keith Rielage, Nicholas Ruof, Danielle Schaper, David Tedeschi, Jared Thompson, Robert Varner, Sergey Vasilyev, Jackson Waters, John Wilkerson, Clint Wiseman, Wenqin Xu, Chang-Hong Yu, Brian Zhu

This material is supported by the U.S. Department of Energy, Office of Science, Office of Nuclear Physics, the Particle Astrophysics and Nuclear Physics Programs of the National Science Foundation, and the Sanford Underground Research Facility.